In Situ Scanning-Tunneling-Microscope Observation of Roughening, Annealing, and Dissolution of Gold (111) in an Electrochemical Cell

Dennis J. Trevor, Christopher E. D. Chidsey, and Dominic N. Loiacono
AT&T Bell Laboratories, Murray Hill, New Jersey 07974
(Received 1 December 1988)

We report *in situ* scanning tunneling microscopy at atomic-layer resolution of the topographic changes accompanying electrochemical reactions. In dilute perchloric acid, Au(111) terraces roughen during the electrochemical formation and reduction of more than a monolayer of gold oxide, but anneal in minutes at moderate potential. Trace chloride enhances step motion, prevents the observation of roughening, and promotes the dissolution of gold during oxidation and rereduction. These observations illustrate the role adsorbates have in determining the surface mobility of substrate atoms.

PACS numbers: 61.16.Di, 66.30.Lw, 81.60.Bn, 82.45.+z

The microscopic details underlying important interfacial electrochemical processes such as electron transfer, plating, passivation, and corrosion are traditionally inferred from *in situ* measurements of macroscopic quantities: charge, potential, concentrations, surface tension, etc. Recently, various groups have demonstrated the feasibility of using *ex situ* electron spectroscopies, microscopies, and diffraction techniques[1-5] and *in situ* techniques such as glancing angle x-ray absorption and diffraction[6-8] and infrared reflection-absorption spectroscopy[9] to obtain structural information about the electrochemical interface at the atomic level. Scanning tunneling microscopy (STM) could offer a microscopic, real-space view of the electrochemical interface to complement these other tools.[10] One immediate target for investigation with the STM is the growth, dissolution, or rearrangement of crystalline surfaces due to electrochemical reactions. A prototypical example of electrochemically induced change at a crystalline surface is the electrochemical oxidation and rereduction of gold.[11-16] Recently, Wiechers *et al.* have demonstrated resolution of monatomic gold layers at the interface of Au(111) and aqueous solutions while controlling the electrochemical potential of the gold surface.[17] Here, we report the first *in situ* STM observations with atomic-layer resolution of the consequences of an electrochemical surface reaction: the roughening, annealing, and dissolution accompanying the oxidation and rereduction of the Au(111) surface.

Gold (111) films on mica were prepared by evaporation of gold onto mica at 225 °C as reported earlier.[18] The samples were clamped to the base plate of a Nanoscope I STM (Digital Electronics) with a Teflon ring, which also formed the electrochemical cell. The counter electrode was a Pt wire, and the reference electrode was an Ag wire in an $AgClO_4$ solution separated from the cell by a length of Teflon tubing. All electrochemical potentials are reported with respect to the normal hydrogen electrode (NHE). $HClO_4$ was Ultra grade (Hopkin and Williams Co.), HCl was reagent grade, water was from a Milli-Q purification train (Millipore Corp.), and oxygen was not removed from the cell. The sample potential was controlled relative to the reference electrode by driving the potential of the counter electrode, and the tip-to-sample bias was fixed at -10 mV.

The tunneling tips were electrochemically etched from platinum/iridium (80:20) wire,[18] dip coated with a silicone polymer, Hipec 648 (Dow-Corning), and baked at 300 °C for 12 h followed by a second dip and second bake at 300 °C for 4 h. To yield stable tunneling images, the tips required brief etching in dilute HF solution to remove the coating at the end. The steady-state electrochemical current at these tips was less than 100 pA from +0.6 to +1.4 V vs NHE. STM images were acquired at a constant tunneling current of 1 nA and a tip bias of -10 mV with respect to the sample. The 2000×2000-Å^2 (100×100 pixel) STM images shown here were acquired at 4000 Å/s (acquisition time 2 min per image).

Figure 1(a) shows a typical image of the surface of a Au(111) thin film on mica in 0.1*M* $HClO_4$ at +0.7 V vs NHE. Note the series of monatomic steps and the large features in each of the lower corners of the image. The large features are associated with a grain boundary in the film just at the edge of the field of view; they were useful for ensuring that subsequent images were acquired at the same place on the sample. The images that we have acquired at +0.7 V are all similar to images of the same samples in air.[18] The location and shape of the step edges and other small features are more readily seen in gray-scale plots of the first derivative of the height with respect to the x axis. Figure 1(b) shows such a presentation of the same data that are in Fig. 1(a). This presentation gives the illusion of viewing the surface from above with illumination from the right.

Figure 2(a) shows current versus potential plots in which the electrochemical potential of a gold sample was scanned at 20 mV/s from +0.7 V vs NHE to +1.7 V (solid) or +2.0 V (dashed) and back to +0.7 V in 0.1*M* $HClO_4$.[19] The two peaks at +1.25 and +1.45 V have been attributed to the formation of a monolayer of gold

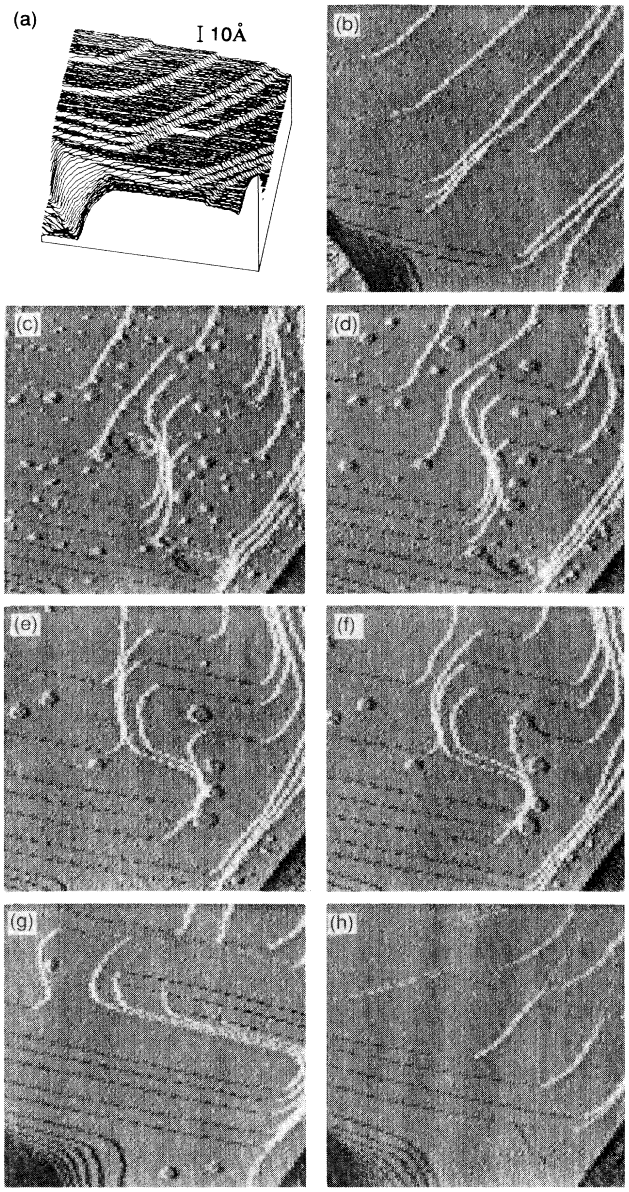

FIG. 1. STM images of one 2000×2000-Å^2 region of a 1400-Å-thick Au(111) film on mica at +0.7 V vs NHE in 0.1M $HClO_4$. (a) Before cycling the electrochemical potential; (b) same image as (a) but presented as a gray-scale map of dz/dx; (c) after cycling to +1.9 V and back to +0.7 V at 20 mV/s. (d) 5 min later; (e) 13 min later; (f) 17 min later; (g) 38 min after cycling to +2.0 V; (h) 15 min after adding dilute HCl to make the electrolyte $5\times10^{-5}M$ HCl, 0.1M $HClO_4$ (Ref. 20).

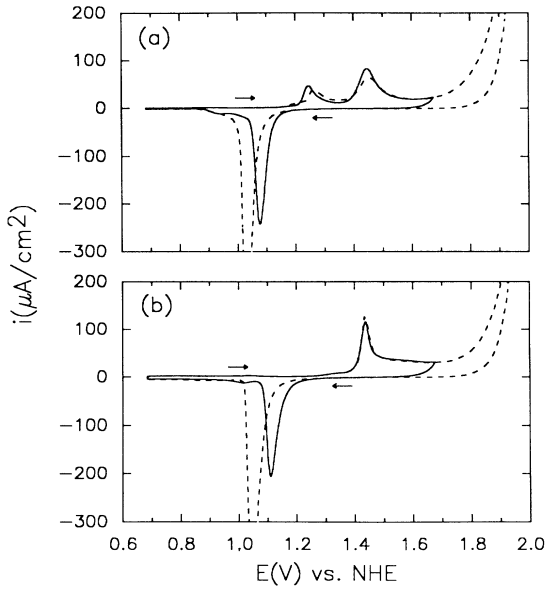

FIG. 2. Current vs potential plots for scans from +0.7 V to +1.7 V (solid) or +2.0 V (dashed) and back to +0.7 V at 20 mV/s. The scans to +2.0 V were preceded by scans to +1.9 V (not shown). (a) 5000-Å-thick Au(111) film on mica in 0.1M $HClO_4$; (b) a same sample as in (a) in $5\times10^{-5}M$ HCl, 0.1M $HClO_4$.

hydroxide and oxide, respectively, so that at +1.7 V, there is approximately a monolayer of gold oxide on the surface.[16] The negative peak near +1.05 V is the "oxide-stripping peak" at which the surface is rereduced to elemental gold. The rise in the dashed line at the positive end of the scan (exceeding the scale of the plot) is due to the onset of the formation of molecular oxygen by the oxidation of water. The gold oxide layer grows thicker than a monolayer in this region as is seen by the increase in the area under the subsequent oxide-stripping peak.

We now continue with the set of experiments illustrated in Fig. 1. After acquiring the image shown in Figs. 1(a) and 1(b), the tip was retracted 200 Å and the sample potential was cycled to +1.6 V vs NHE and back to +0.7 V at mV/s. No roughening of the terraces was seen in a subsequent image. Cycling to +1.7 V left only a few very small pits in the terraces which disappeared in less than 3 min. Cycling to +1.8 V left a low density of pits 40 Å or less in diameter in the terraces. These almost completely disappeared in less than 10 min. Cycling to +1.9 V resulted in the image shown in Fig. 1(c). The pits are more numerous and larger in diameter than those formed in the cycle to +1.8 V. Where they are large enough to be resolved, the pits are 1 monolayer deep. There is also a new protruding feature just left of the center of the image. It is three new terraces, one atop the other. Such protruding features are more rare than the pits, but we have observed them in many images. As before, the roughness disappeared with time. At first, the smaller pits disappear, apparently fusing with terrace edges and with each other to form larger pits [compare Figs. 1(c) and 1(d)]. After 13 min, only a few relatively large pits remain in Fig. 1(e). These larger pits also decrease in number with time. Figures

1(e) and 1(f), obtained 4 min apart, show an example of how the large pits disappear. The large pit just above and right of center in Fig. 1(e) fused with the next lower terrace to give the highly curved step edge in Fig. 1(f). A subsequent image showed that the step edge straightened out to a broadly rounded shape.

Following the annealing shown in Figs. 1(c) through 1(f), the surface was next cycled to +2.0 V vs NHE and back to +0.7 V. Initially, the topography was so rough that the original step edges were hard to pick out. After about 4 min, the step edges were again apparent and a high density of pits in the terraces was seen. As before the surface roughness annealed with time. Figure 1(g) shows the surface after all but three of the pits were gone; note that the potential cycles left the step edges following quite convoluted paths. This highly curved step topography was relatively stable until a small amount of dilute HCl was added to the cell to make the electrolyte $5\times10^{-5}M$ in HCl. In much less than 15 min, the steps had straightened out as shown in Fig. 1(h).[20] Note the resemblance of Figs. 1(b) and 1(h). Adsorbed chloride apparently enhances step motion. A similar observation of the effect of chloride on step motion has been reported by others.[17]

Several experiments similar to that outlined above have shown that, in $0.1M$ $HClO_4$, cycles to potentials at which less than 1 monolayer of gold oxide is formed do not result in a roughening of the surface. However, cycles to higher potentials at which more than a monolayer of oxide is formed, result in roughened terraces which then anneal at moderate potential. The annealing of the roughness is not the result of the tip scanning just above the surface because longer times between scans result in a greater degree of smoothing. We speculate that the roughening that we observe is the consequence of place exchange reactions of gold and oxygen, which must occur whenever more than a monolayer of oxide is formed or reduced. The substantial hysteresis shown in Fig. 2(a) between the electrochemical potential of the bulk oxidation and reduction (>0.7 V) suggests that large numbers of energetic species such as adatoms and vacancies could be formed during reduction of the oxide. The excess energy of these species would then dissipate as they found each other and step edges.

We turn now to the effect of chloride. As we saw in Fig. 1(h), adding chloride after roughening the surface accelerates the annealing. Figure 2(b) shows current versus potential plots in $5\times10^{-5}M$ HCl, $0.1M$ $HClO_4$. From the change in peak positions from Fig. 2(a) to 2(b), it is clear that chloride anion adsorption plays a significant role in the energetics of the gold oxidation process.[12]

Figure 3 illustrates the topographic changes accompanying such potential cycles. The image in Figs. 3(a) and 3(b) was obtained after cycling to +1.6 V. No change had occurred in the positions or paths of the step edges as a result of the potential cycle. Note the emergent points of two dislocations,[18] one above the other, in Figs. 3(a) and 3(b). These dislocations provide two useful fixed points on the surface from which the motion of steps can be judged. Figure 3(c) shows the result of a potential cycle to +1.9 V. The three steps in Fig. 3(b) have each moved a bit to the left. Two more cycles to +1.9 V caused the steps to move back more. Finally, Fig. 3(d) shows the result of three cycles to +2.0 V. Note that the higher step now originates from the dislocation lower in the picture. This exchange is the geometrical consequence of the middle terrace dissolving away until the lower step passes across the upper dislocation.

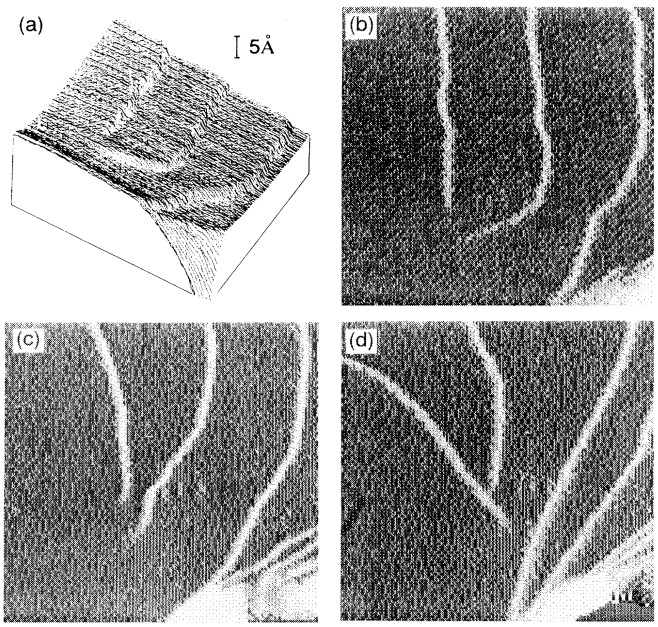

FIG. 3. STM images of one 2000×2000-Å^2 region of a 1400-Å-thick Au(111) film on mica at +0.7 V vs NHE in $5\times10^{-5}M$ HCl, $0.1M$ $HClO_4$ showing the emergent points of two dislocations. (a) After cycling to +1.6 V and back to +0.7 V at 20 mV/s; (b) same image as (a) but presented as a gray-scale map of dz/dx; (c) after cycling to +1.9 V; (d) after three cycles to +2.0 V.

Within the region shown in Fig. 3, about half a monolayer of gold appears to have been lost by dissolution. In contrast, similar losses of gold have not been noted in the absence of chloride. A further difference which distinguishes the STM images in chloride-containing electrolyte from those in chloride-free electrolyte is the lack of evidence of roughening of the terraces after formation and rereduction of more than a monolayer of gold oxide. This could be because such roughening does not occur or because the annealing of the roughening is much faster in the presence of chloride. The occurrence of hysteresis between the oxide formation and reduction features in Fig. 2(b) and the enhanced mobility of steps shown in

Fig. 1(h) lead us to infer that roughening does occur in chloride-containing solution but that the annealing is too fast to observe.

The roughening of gold by oxidation and rereduction in perchlorate solutions has been inferred from macroscopic measurements of current-potential curves. Furthermore, the surface appears to return eventually to its initial state.[11] Our microscopic measurements not only confirm the inferred roughening and provide a real-space image of that roughness, but also are much more sensitive to the onset of roughness. As an example, note that while cycling the sample potential to +1.9 V vs NHE slightly changes the shape of the oxidation peaks in Fig. 2(a), the same potential cycle dramatically changes the surface topography in Fig. 1(c). Though one might be reluctant to draw a conclusion from the change in the voltammetry, the STM images are unambiguous, and clearly show the potential utility of *in situ* STM studies in which monatomic layers are resolved.

Comparison of surface annealing under various conditions illustrates the role of adsorbates in determining surface-atom mobility. In UHV, the annealing of surface features on Au(111) has been followed with STM by Jaklevic and Elie.[21] They created pits a few monolayers deep by mechanically indenting the surface with the tip and watched as the pits filled in slowly over hours. In the presence of aqueous perchlorate, a weakly adsorbed anion, we see monatomic pits of a similar diameter, created in our case by oxidation and rereduction cycles. These pits appear to move about and fuse with each other and step edges; they are not stable for the hours over which the mechanically formed pits are stable. In the presence of aqueous chloride, a strongly adsorbed anion, no pits are seen at all on the time scale of the experiment (about a minute), and there is evidence for the rapid motion of step edges. The rate of annealing in these three situations correlates with the degree of adsorption at the surface. This correlation can be explained by postulating that the bonding of surface gold atoms to adsorbates reduces the strength of the bonds to neighboring gold atoms, increasing the atom mobility. Recent entended x-ray absorption fine-structure work by Sette *et al.* provides structural support for this idea. The Debye-Waller factors of metal-metal distances at the Cu(001) and Ni(001) surfaces in UHV increase when Cl or S is adsorbed,[22] a manifestation of the weakening of substrate-substrate bonds due to adsorption.

In summary, STM can be used to study chemical change with atomic-layer resolution at the electrochemical interface. 1-monolayer-deep pits are created in the Au(111) surface by electrochemical oxidation and rereduction in the absence of chloride. The pits grow by fusion and migrate to step edges on the time scale of minutes at room temperature. In chloride-containing solutions, the mobility of surface atoms is greatly enhanced and dissolution of gold occurs during oxidative potential cycles.

[1]A. T. D'Agostino and P. N. Ross, Surf. Sci. **185**, 88 (1987).

[2]A. T. Hubbard, Chem. Rev. **88**, 633 (1988).

[3]J. Canullo, Y. Uchida, G. Lehmpfuhl, T. Twomey, and D. M. Kolb, Surf. Sci. **188**, 350 (1987).

[4]S. Haupt, U. Collisi, H. D. Speckmann, and H.-H. Stehblow, J. Electroanal. Chem. **194**, 179 (1985).

[5]J. P. Bellier, J. Lecoeur, and A. Rousseau, J. Electronanal. Chem. **200**, 55 (1985).

[6]M. G. Samant, M. F. Toney, G. L. Borges, L. Blum, and O. R. Melroy, J. Phys. Chem. **92**, 220 (1988).

[7]J. H. White, M. J. Albarelli, H. D. Abruna, L. Blum, O. R. Melroy, M. G. Samant, G. L. Borges, and J. G. Gordon, J. Phys. Chem. **92**, 4432 (1988).

[8]M. Fleischmann and B. W. Mao, J. Electroanal. Chem. **247**, 297 (1988).

[9]K. Ashley and S. Pons, Chem. Rev. **88**, 673 (1988).

[10]R. Sonnenfeld, J. Schneir, and P. K. Hansma, in "Modern Aspects of Electrochemistry," Vol. 21, edited by J. O'M. Brockris (to be published), and references therein.

[11]D. Dickertmann, J. W. Schultze, and K. J. Vetter, J. Electoanal. Chem. **55**, 429 (1974).

[12]S. H. Cadle and S. Bruckenstein, J. Electroanal. Chem. **48**, 325 (1973).

[13]S. H. Cadle and S. Bruckenstein, Anal. Chem. **46**, 16 (1974).

[14]S. Bruckenstein and M. Shay, J. Electroanal. Chem. **188**, 131 (1985).

[15]R. Schumacher, G. Borges, and K. K. Kanazawa, Surf. Sci. **163**, L621 (1985).

[16]H. Angerstein-Kozlowska, B. E. Conway, A. Hamelin, and L. Stoicoviciu, J. Electroanal. Chem. **228**, 429 (1987).

[17]J. Wiechers, T. Twomey, D. M. Kolb, and R. J. Behm, J. Electroanal. Chem. **248**, 451 (1988).

[18]C. E. D. Chidsey, D. N. Loiacono, T. Sleator, and S. Nakahara, Surf. Sci. **200**, 45 (1988).

[19]The voltammetry in Fig. 2 was obtained with a thicker sample than those used for STM and in a cell that was more convenient to use than the STM cell. In the STM cell, the two anodic peaks were not as well resolved, possibly due to trace impurities in the cell or to the higher step densities at the more open grain boundaries in the thinner samples (Ref. 18).

[20]The point on the tip drawing tunneling current appears to be different in the upper-right-hand corner of this image than in the rest of the image. Tip changes, ghost images, and changes in tip resolution, though not a continuous problem, are a common artifact in these experiments.

[21]R. C. Jaklevic and L. Elie, Phys. Rev. Lett. **60**, 120 (1988).

[22]F. Sette, T. Hashizume, F. Comin, A. A. MacDowell, and P. H. Citrin, Phys. Rev. Lett. **61**, 1384 (1988).

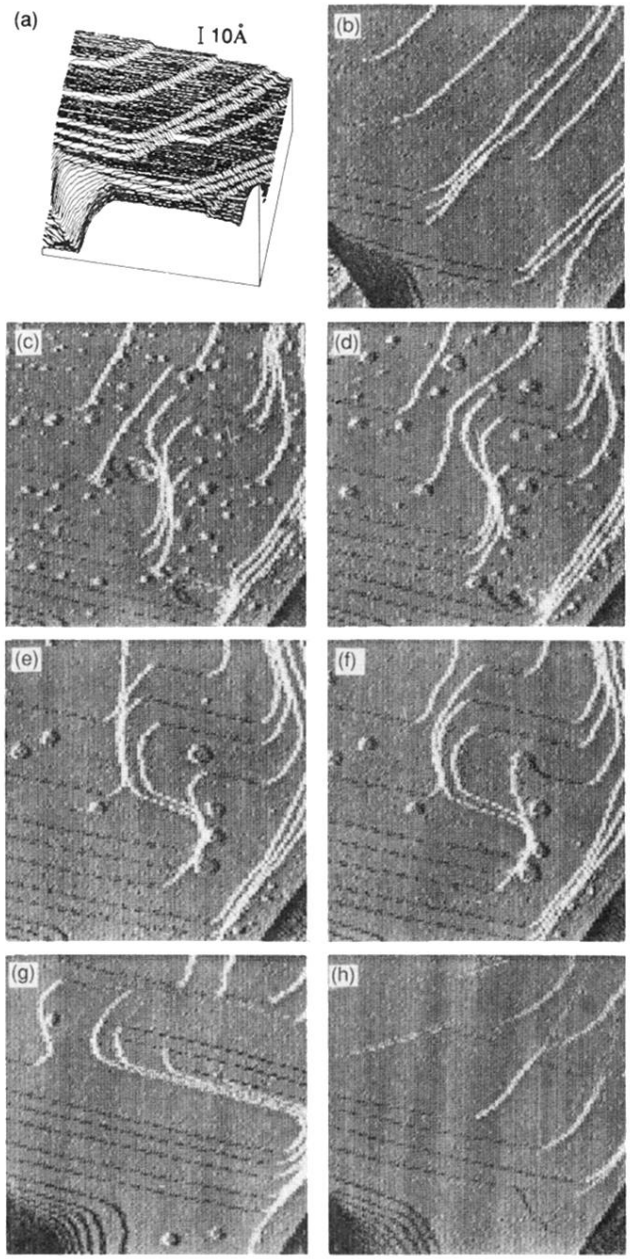

FIG. 1. STM images of one 2000×2000-Å^2 region of a 1400-Å-thick Au(111) film on mica at +0.7 V vs NHE in $0.1M$ $HClO_4$. (a) Before cycling the electrochemical potential; (b) same image as (a) but presented as a gray-scale map of dz/dx; (c) after cycling to +1.9 V and back to +0.7 V at 20 mV/s. (d) 5 min later; (e) 13 min later; (f) 17 min later; (g) 38 min after cycling to +2.0 V; (h) 15 min after adding dilute HCl to make the electrolyte $5\times10^{-5}M$ HCl, $0.1M$ $HClO_4$ (Ref. 20).

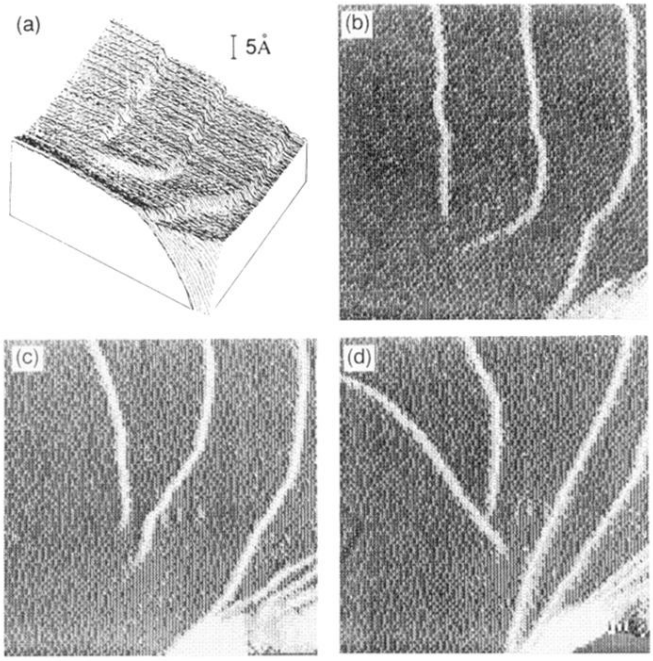

FIG. 3. STM images of one 2000×2000-Å^2 region of a 1400-Å-thick Au(111) film on mica at +0.7 V vs NHE in $5\times10^{-5}M$ HCl, $0.1M$ $HClO_4$ showing the emergent points of two dislocations. (a) After cycling to +1.6 V and back to +0.7 V at 20 mV/s; (b) same image as (a) but presented as a gray-scale map of dz/dx; (c) after cycling to +1.9 V; (d) after three cycles to +2.0 V.